SPINE Volume 34, Number 21, pp 2288–2296

The Morphology of Acute Disc Herniation

A Clinically Relevant Model Defining the Role of Flexion

Samuel P. Veres, BEng,* Peter A. Robertson, MD,† and Neil D. Broom, PhD*

Study Design. Hydrostatically induced disruption of flexed lumbar intervertebral discs followed by microstructural investigation.

Objective. To investigate how flexion affects the anulus' ability to resist rupture during hydrostatic loading, and determine how the characteristics of the resulting disc failures compare with those observed clinically.

Summary of Background Data. While compression of neutrally positioned motion segments consistently causes vertebral failure, compression of flexed segments can induce herniation. Why flexion has this effect remains unclear. A vast range of herniation characteristics have been documented clinically; whether flexion-related herniations are likely to possess a subset of these is unknown.

Methods. Forty-two ovine lumbar motion segments, dissected from the same 3 levels of 14 spines, were each flexed 7° or 10° from the neutral position. While maintained at one of these angles, the nucleus of each segment was gradually injected with a viscous radio-opaque gel *via* an injection screw placed longitudinally within the inferior vertebra, until failure occurred. Each segment was then inspected using microcomputed tomography and oblique illumination microscopy in tandem.

Results. Eighteen segments suffered disc failure; 14 of these were caused by direct radial rupture of the anular wall. All radial ruptures were located in the central posterior anulus. Nine radial ruptures contained nuclear material, which had breached the posterior longitudinal ligament in 1 disc, and reached it in 5 others forming transligamentous and subligamentous nuclear extrusions, respectively. The most common radial rupture route, occurring in 10 discs, involved a systematic anulus-endplate-anulus failure pattern.

Conclusion. Flexion places the anulus at risk by facilitating nuclear flow, limiting circumferential disruption while promoting radial rupture, and rendering the endplate/vertebra junction vulnerable to failure. Flexion may play a developmental role in those herniations possessing a central posterior radial rupture that incorporates a short span of endplate disruption along the apex of the vertebral rim.

Key words: lumbar, intervertebral disc, flexion, herniation, prolapse, extrusion, microscopy, microstructure.
Spine 2009;34:2288–2296

Flexion of the spine and lumbar disc herniation have a long-standing association. It was common for patients who presented with some of the earliest surgically confirmed cases of symptomatic herniations to recall a definitive traumatic event involving either lifting[1] or, more generally, flexion[2] coinciding with the onset of their pain.

Prompted by the anecdotal evidence provided by presenting patients, Adams and Hutton investigated the effect of compressing cadaveric discs positioned in hyperflexion.[3] Unlike earlier studies involving the mechanical compression of neutrally positioned motion segments, which consistently resulted in vertebral rather than disc failure,[4–7] herniation occurred in roughly half of Adams and Hutton's hyperflexed discs.

To date, several attempts have been made to induce herniation *in vitro* using complex mechanical loading scenarios involving flexion. Flexion and compression,[3,8] flexion with cyclic compression,[9,10] and cyclic flexion/extension with light or no compression[11–15] have all been employed with varying degrees of success.

Clinically, discography and histology have provided an increased understanding of the range of herniation morphologies that can occur. Herniations are commonly divided into 2 groups: protrusions and extrusions.[16] Protrusions can occur with or without nuclear involvement.[17,18] Extrusions can be subligamentous, transligamentous, or sequestered.[17,19] Herniation routes commonly occur in the central posterior, paracentral posterior, and posterolateral anulus,[20,21] and may track superiorly, inferiorly, or at mid-disc height.[21] Herniated material can include nucleus, anulus, and endplate, alone or in combination.[18,19,22,23]

Given that flexion does play a developmental role in some herniations, a hypothesis that is now supported by more formal epidemiologic evidence,[24,25] how do those created in the laboratory compare with those observed clinically? Which of the numerous clinically observed herniation characteristics is a flexion-related injury likely to possess? How does flexion render discs vulnerable to rupture?

For *in vitro* herniation studies to help answer these questions, adequate clinical comparisons must be made. This necessitates a detailed morphologic examination of the ruptures created *in vitro*. Although preliminary studies of this nature have been conducted,[14,15] clinically relevant herniations created using physiologic levels of flexion have yet to be thoroughly detailed.

In the current study we have created herniations using modest levels of flexion combined with nuclear pressurization. The anular ruptures created have been studied using microcomputed tomography (micro-CT) and microscopy in tandem. Comparing these results with those from previously inflated neutral discs[26] has allowed us to

From the *Department of Chemical and Materials Engineering, University of Auckland, Auckland, New Zealand; and †Department of Orthopaedic Surgery, Auckland Hospital, Auckland, New Zealand.
Acknowledgment date: November 9, 2009. Acceptance date: January 15, 2009.
The manuscript submitted does not contain information about medical device(s)/drug(s).
Corporate/Industry, Federal, and Foundation funds were received in support of this work. No benefits in any form have been or will be received from a commercial party related directly or indirectly to the subject of this manuscript.
Address correspondence and reprint requests to Neil D. Broom, PhD, Department of Chemical and Materials Engineering, University of Auckland, Auckland, New Zealand; E-mail: nd.broom@auckland.ac.nz

determine how flexion affects the anulus ability to resist rupture. The morphologic details of these *in vitro* herniations will allow higher-level comparisons to be drawn with future clinical observations and *in vitro* studies.

■ Materials and Methods

Fourteen freshly harvested ovine lumbar spines, aged 2 to 5 years, were wrapped in plastic film and stored at −20°C for no more than 3 months. Each spine was randomly assigned to 1 of 2 test groups: 7° flexion or 10° flexion. In preparation for testing, each spine was removed of extraneous soft tissues and posterior elements as previously described.[26] The L1–L2, L3–L4, and L5–L6 motion segments were isolated from each spine by bisecting the discs above and below. Each bisected disc was visually inspected; no macroscopic ruptures, clefts, or areas of discoloration were found. Before testing, each motion segment was soaked for 20 hours in 0.15 M saline at 4°C to ensure a consistent level of hydration.

Following the method of Schechtman *et al*,[27] a self-tapping injection screw (major thread diameter 4.5 mm, internal bore diameter 1.5 mm) was inserted longitudinally through the inferior vertebra of each motion segment so that its tip contacted the center of the nucleus. Using dental plaster, each segment's vertebrae were then potted in stainless steel rings in such a way that the 2 rings and inferior vertebra were coaxial. During this process, the exterior of the intervening disc was wrapped in saline soaked gauze covered by plastic film to prevent dehydration.

A bench-top rig was used to flex each potted segment about a fixed axis running perpendicular to the sagittal plane and passing through the nucleus at mid-disc height. Each segment was gradually flexed (approximately 0.02°/s) to its assigned limit of either 7° or 10° from the neutral position. Using a quick release coupling, the injection screw was connected to a manually actuated piston-cylinder device containing a viscous radio-opaque gel described previously.[26] At this point the saline soaked gauze covering the disc's exterior was removed to allow visual monitoring during the injection process.

The pressure within each disc's nucleus was gradually increased in a ramp-and-hold manner by advancing the piston 0.3 mm at a rate of 0.008 to 0.012 mm/s and then waiting 12 to 14 seconds before the next advance. Injection was halted and the intradiscal pressure immediately relieved when either: (i) a focal change in the disc's periphery was observed, (ii) material extruded from the periphery, or (iii) there was a sudden drop in nuclear pressure. During testing, the pressure of the injected gel was monitored using a pressure transducer (model LM/2345–6, Sensotec, US; ±0.3 MPa accuracy) positioned at the base of the injection screw, and recorded at a rate of 2 Hz using a data acquisition system (data logger model TC-08, PicoLog software version 5.13.4; Pico Technology, UK).

Following removal of the injection screw, each motion segment's vertebrae were transected leaving approximately 5 mm of bone attached to both ends of the disc. These trimmed segments were immediately wrapped in plastic film and frozen at −20°C. Each segment was imaged at a resolution of 34.6 μm using a micro-CT scanner (model 1172, SkyScan, Belgium) operating at 100 kV/100 μA and subsequently processed into axial and sagittal image sets using NRecon and DataViewer software (version 1.5.0.2 and 1.5.0.2, SkyScan).

Following micro-CT, each segment was fixed in 10% formalin and then decalcified in 10% formic acid. Using a scalpel, each segment was bisected in the coronal plane. Two oblique cuts, running along the anular fiber direction, were used to remove a large central posterior block. Using a freezing-sledging microtome, the posterior block of each segment was cut into approximately 100 oblique radial bone-disc-bone cryosections, each 30 μm thick. Cryosections were wet-mounted and examined unstained using oblique illumination microscopy. In the limited number of cases where micro-CT images indicated posterolateral or anterior disruption, these additional regions were also microscopically inspected.

In order to ensure that the flexion process itself was not causing any damage to the discs, the L1–L2, L3–L4, and L5–L6 motion segments of three additional spines were tested as controls. These segments were taken through the same experimental procedure as the 10° flexion group, but no contrast gel was injected into the nucleus. Posterior cryosections from each disc were examined microscopically.

Statistics were computed using SPSS software (version 12.0.1). Mean failure pressures were compared using *t* tests. Categorical group-outcome correlations were tested for significance with 2-tailed *P*-values calculated using Fisher exact test.

■ Results

Nine motion segments were tested as controls at an angle of 10° to ensure that the flexion process alone did not damage discs. No tissue disruption within any of these 9 discs was observed during the microscopic examination of posterior cryosections.

Twenty-one motion segments were tested in each of the 7° and 10° flexion groups. Peak rates of pressurization ranged from 0.04 to 0.10 MPa/s. Nuclear gel injection failed in 8 segments, 4 from each group, due to gel leakage at the inferior endplate/screw interface. These samples exhibited both abnormal pressure-time responses and large inferior vertebra/disc gel content fractions. Following inspection by micro-CT, the remaining 34 segments were each classified as either a vertebral or disc failure and then further subclassified after microscopic investigation. Herniations were classified as nuclear extrusions if nuclear material had breached the outer anular wall. Failure data for the 34 successfully pressurized segments are listed in Table 1.

Because the age of each spine was not available, the maturity of each motion segment was assessed by documenting the status of its growth plates as observed on central posterior cryosections. Growth plates, which ossify with age, were recorded as open, partially fused, or fused (Table 1). No significant correlation was found between motion segment maturity and failure mode.

Vertebral Failures

Sixteen segments suffered vertebral failure, 6 in the 7° group and 10 in the 10° group (Table 1). Ten failures occurred adjacent to the center of the nucleus; 8 of these were located at the inferior vertebra/screw junction. Although the presence of the injection screw may have played a role in failure of these samples, they did not exhibit the abnormal pressurization characteristics mentioned above, and thus could not be discounted as technical failures.

In 6 segments a crescent-shaped piece of bone was separated from the outer central posterior portion of one

Table 1. Failure Data for Ovine Lumbar Motion Segments Successfully Pressurized While Flexed

Failure Mode	Segment (Angle–Spine–Disc)	Site of Gel Extrusion	Detailed Failure Mode	Failure Pressure (MPa)	Growth Plate Status
Vertebral	7–1-L34	SV	Cen (SV)	10.6	O
	7–5-L34	SV	Cen (SV)	14.0	O
	7–2-L34	IV	Cen (IV)	8.7	O
	7–3-L34	IV	Cen (IV)	7.6	F
	7–2-L56	IV	Rim (IV)	8.8	O
	7–2-L12	CP	Rim (IV)	10.6	O
	Mean ± SD			10.1 ± 2.3	
Disc	7–5-L56	PP	Diff	15.8	O
	7–6-L56	PP	Diff	13.3	O
	7–6-L34	PP	Diff	13.9	O
	7–7-L56	PP	MA	8.4	F
	7–7-L34	PL	MA	9.8	F
	7–1-L12	CP & PL	MA–SNE	13.0	O
	7–7-L12	CP	MA–SNE	11.8	F
	7–1-L56	PP	A/E (IV)–NF	10.1	O
	7–4-L12	CP	A/E (IV)–NF	8.3	P
	7–4-L56	CP	A/E (IV)–SNE	11.1	F
	7–4-L34	CP	A/E (SV)–TNE	8.2	P
	Mean ± SD			11.2 ± 2.5	
Vertebral	10–8-L56	IV	Cen (IV)	7.7	O
	10–9-L56	IV	Cen (IV)	7.0	F
	10–9-L12	IV	Cen (IV)	9.5	P
	10–12-L34	IV	Cen (IV)	5.5	O
	10–14-L34	IV	Cen (IV)	11.5	O
	10–14-L12	IV	Cen (IV)	8.3	O
	10–10-L34	PP	Rim (SV)	14.3	F
	10–10-L12	CP & PL	Rim (SV)	15.1	F
	10–11-L34	CP	Rim (IV)	10.6	O
	10–11-L12	IV	Rim (IV)	9.9	O
	Mean ± SD			9.9 ± 3.1	
Disc	10–12-L56	PP	Diff	13.3	O
	10–9-L34	PP	A/E (SV)	11.7	P
	10–8-L12	PL	A/E (IV)	6.6	O
	10–13-L56	PP	A/E (IV)	9.7	F
	10–10-L56	CP	A/E (IV)–NF	6.1	F
	10–11-L56	CP	A/E (SV)–SNE	10.7	P
	10–14-L56	CP	A/E (IV)–SNE	10.4	P
	Mean ± SD			9.8 ± 2.6	

PP indicates paracentral posterior anulus; CP, central posterior anulus; PL, posterolateral anulus; Cen, central; Rim, rim fracture; Diff, diffuse anular rupture; MA, radial mid-axial anular rupture; A/E, radial anular-endplate rupture; SV, superior vertebra; IV, inferior vertebra; NF, nuclear flow through rupture; SNE, subligamentous nuclear extrusion; TNE, transligamentous nuclear extrusion; O, open; P, partially fused; F, fused.

vertebral endplate. These were classified as rim fractures. In these segments, the vertebral endplate had failed adjacent to the inner to mid posterior anulus. From this point the fracture propagated near the cortical/cancellous bone interface, spreading an average of 6.5 mm circumferentially, and extending radially to the posterior periphery (Figure 1).

Disc Failures

Eighteen segments suffered disc failure, 11 in the 7° group and 7 in the 10° group (Table 1). The mean failure pressures of these two groups were not significantly different. No significant correlations were found between segment maturity and detailed failure mode or the occurrence of nuclear flow through the anulus.

On failure most segments extruded gel from either the central or paracentral posterior anulus. Qualitatively, the central posterior extrusions were both more sudden and voluminous than the paracentral extrusions. Discs which suffered central posterior extrusions often emitted a sharp snap, whereas those that suffered paracentral extrusions emitted a softer intermittent tearing sound before gel emerged from the disc's periphery. A distinct subligamentous bulge was observed in several discs (Figure 2A), and gently removing the extruded gel revealed a central posterior transligamentous nuclear extrusion in one segment (Figures 2B, C). The extruded nuclear material, like the nucleus of those discs that were bisected when isolating the tested motion segments, was resilient and cohesive; it could

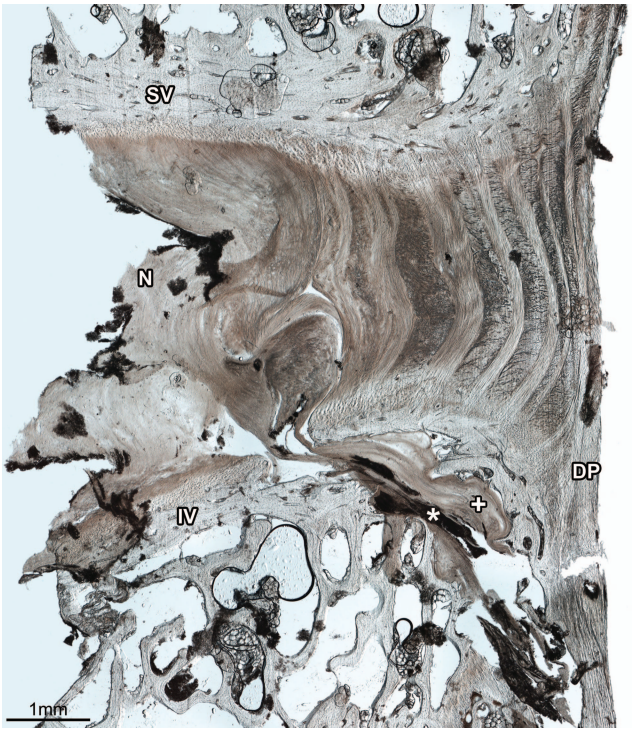

Figure 1. The morphology of a typical posterior rim fracture (segment 7–2-L56 is shown). The inferior vertebral endplate has ruptured adjacent to the inner anulus. The fracture, which contains both contrast gel (*) and nuclear material (+), has propagated radially, near the cortical/cancellous bone junction, to the disc periphery. SV indicates superior vertebra; IV, inferior vertebra; N, nucleus; DP, disc periphery.

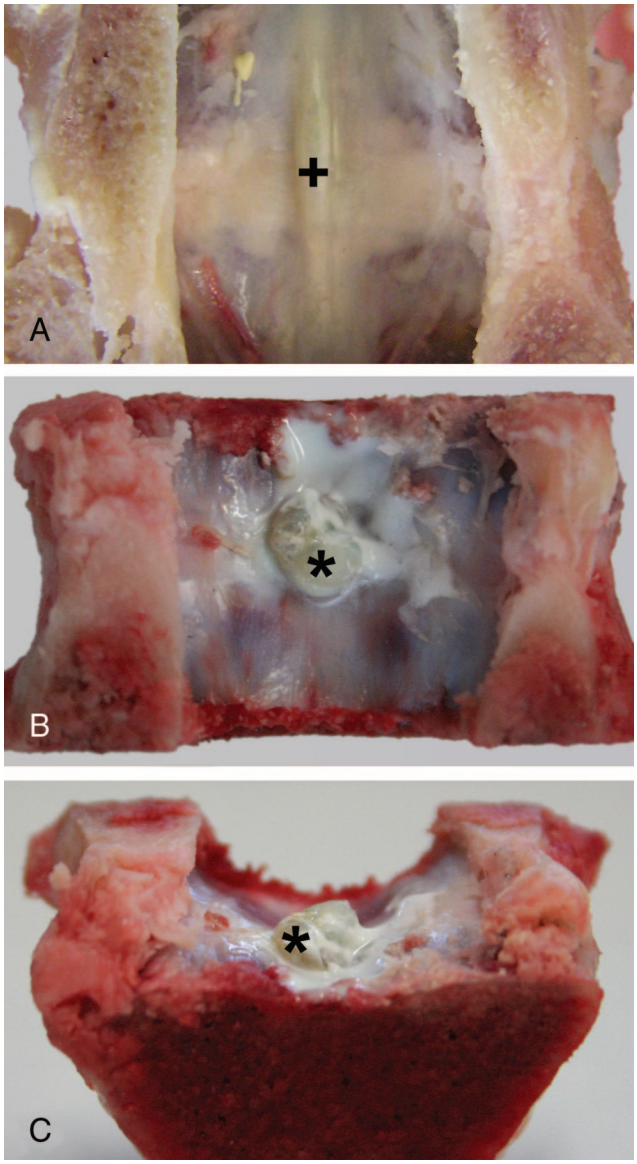

Figure 2. Post-testing photographs show subligamentous (+ in **A**; segment 10–11-L56) and transligamentous (* in **B**, **C**, segment 7–4-L34) nuclear extrusions.

not be described as having the ability to "[flow] under its own weight" as some extrusions have previously.[3] Posterolateral gel extrusions were least common, occurring in only 4 segments (Table 1).

Axial micro-CT projections showed that gel-induced disruption of the posterior anulus occurred in each of the 18 segments. The disruption was highly confined; rarely did gel penetrate the inner anterior, lateral, or posterolateral anular regions. Circumferential gel flow from the inner and mid posterior to the posterolateral anulus was also rare. In discs that had extruded gel from the posterolateral anulus, micro-CT projections showed that gel had reached the point of posterolateral extrusion by tracking circumferentially from the outer posterior anulus, not by radial posterolateral rupture (Figure 3).

Microscopic examination of sequential posterior cryosections from each segment showed that 3 distinct modes of disc failure occurred: diffuse anular rupture, radial mid-axial anular rupture, and radial anular-endplate rupture. While the characteristics of each failure mode were similar between flexion groups, the incidences of each varied as listed in Table 2.

Diffuse rupture of the posterior anulus occurred in 4 of the 18 segments. These ruptures were characterized by large amounts of circumferential gel flow within the posterior anulus, which occurred preferentially within the fiber bundles of lamellae (Figure 4). Some instances of interlamellar disruption were observed, but only in the outer posterior anulus. Radial ruptures were short, usually spanning only a single lamella, and were circumferentially distributed. No endplate disruption or flow of nuclear material occurred in these samples.

Radial mid-axial anular ruptures were the cause of disc failure in 4 segments, all from the 7° flexion group. These ruptures were characterized by a single radially oriented rupture through the entire thickness of the central posterior anular wall in the mid-axial plane. In two cases, a large fragment of nuclear material was found within the rupture that had reached, but failed to breach, the posterior longitudinal ligament (Figure 5). No endplate disruption occurred in these samples.

Radial anular-endplate ruptures were the most common mode of disc failure, occurring in 10 segments. Like

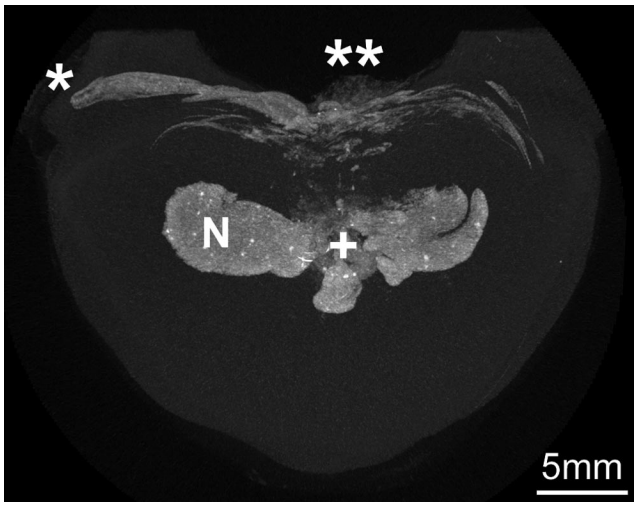

Figure 3. This axial micro-CT projection of segment 7–1-L12 shows only the injected contrast gel and vertebrae. In most discs disruption was largely confined to the posterior anulus. Posterolateral gel extrusions (*) were caused by circumferential gel flow from the outer posterior anulus, not by direct radial rupture from one of the nuclear lobes (N). + marks the site of gel injection; **marks a central posterior extrusion.

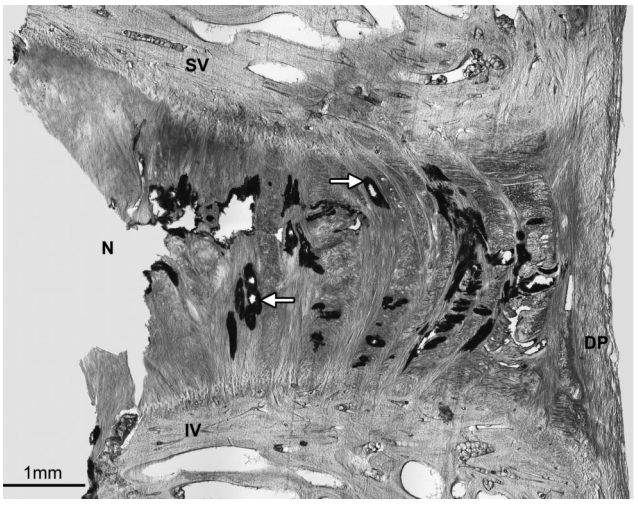

Figure 4. Diffuse rupture of the posterior anulus (segment 7–6-L56 is shown). The preferential mode of gel flow is within anular fiber bundles, which appear as discrete disruptions (arrows) on radial sections. SV indicates superior vertebra; IV, inferior vertebra; N, nucleus; DP, disc periphery.

the radial mid-axial ruptures, these occurred as a single radially oriented rupture though the entire thickness of the central posterior disc wall. Unlike the mid-axial ruptures, the site of tissue failure along the radial length these ruptures consistently changed from anulus to endplate to anulus. The initial anular portion of these ruptures occurred in the mid-axial plane of the inner anulus. At the apex of the vertebral rim, adjacent to the mid-anulus, the rupture shifted from anulus to endplate. At the beginning of the outer anulus, the ruptures shifted back into the mid-axial plane (Figure 6).

The endplate portion of these ruptures, which most often was located inferiorly, always occurred at the cartilaginous/vertebral endplate junction and extended a radial distance of approximately 1 mm (Figure 7). Circumferentially, these endplate ruptures extended an average of 5 mm (range: 1–7 mm), often spreading considerably farther than the anular portion of the rupture (Figure 8).

Fewer of the 10° radial anular-endplate ruptures contained nuclear material than those of the 7° group, however, qualitatively the 10° ruptures contained a larger volume of nuclear material (Figures 9 *vs.* 6). In one 10° segment (10–14-L56), the portion of unanchored anulus adjacent to the endplate rupture was carried out to the disc periphery by a large volume of nuclear material (Figure 9). In this case, nucleus, anulus, and cartilaginous endplate were all extruded from the disc.

Table 2. Incidences of Disc Failure Mode in Flexed and Nonflexed Segments

	Incidences of Disc Failure		
Flexion Angle	Diffuse	Mid-Axial	Anular-Endplate
10°	1	0	6
7°	3	4	4
0°*	5	2	0

*Numerical summary of a portion of the textual results.[26]

■ Discussion

Limited availability and the required ethical processes made the use of healthy human tissue in this study

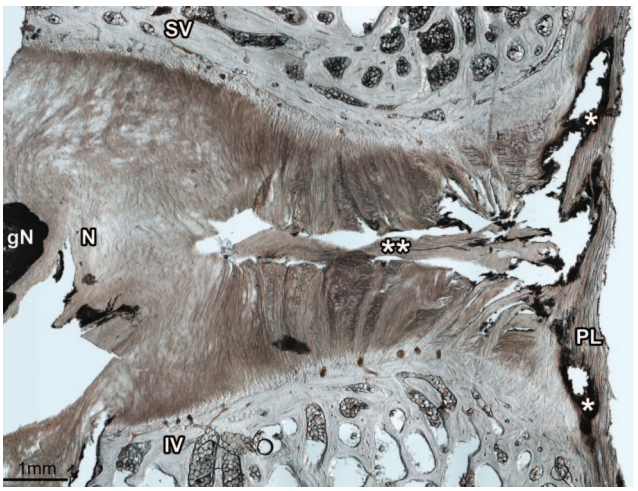

Figure 5. Radial mid-axial anular rupture (segment 7–7-L12 is shown). Compressed nuclear material (**) has bisected the posterior anulus, but has not breached the posterior longitudinal ligament (PL), forming a subligamentous nuclear extrusion. Tissue voids, outlined in residual gel (*), indicate that the injected gel has flowed through this rupture and spread circumferentially between the PL and outer anulus. SV indicates superior vertebra; IV, inferior vertebra; N, nucleus; gN, gel in nucleus.

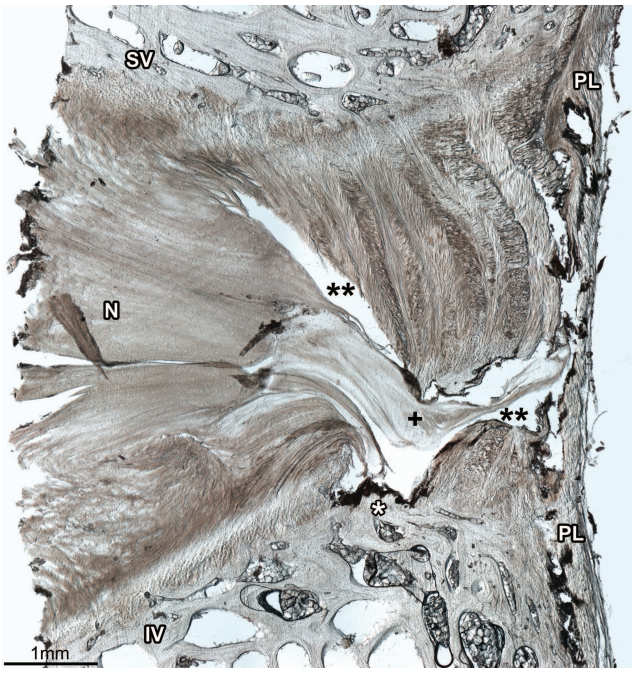

Figure 6. Radial anular-endplate rupture of the posterior anulus (segment 7–4-L56 is shown). This mode of disc failure was characterized by two regions of mid-axial anular rupture (**) connected by an endplate rupture adjacent to the mid-anulus (*). In this disc, nuclear material (+) has reached, but failed to rupture the posterior longitudinal ligament (PL) resulting in a subligamentous nuclear extrusion. SV indicates superior vertebra; IV, inferior vertebra; N, nucleus.

unfeasible. In lieu, ovine lumbar spines have been used, which are similar to human lumbar spines in anatomic structure,[28] biomechanical function,[29,30] and biochemical disc composition.[31]

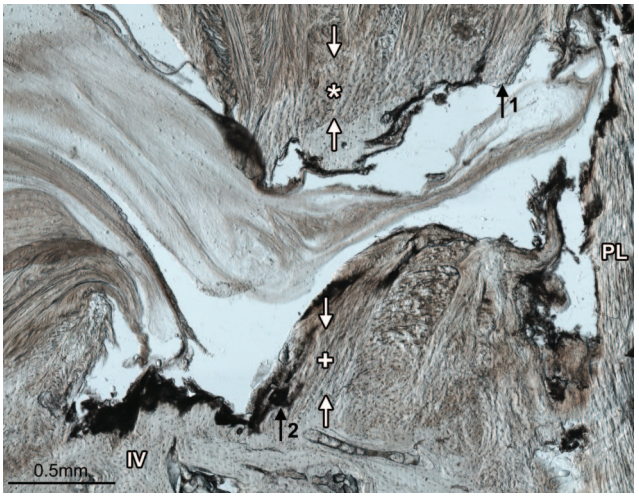

Figure 7. Failure of the endplate in radial anular-endplate ruptures always occurred at the cartilaginous/vertebral endplate junction. The ruptured portion of the junction generally extended a radial distance of roughly 1 mm. The thickness of the cartilaginous endplate is indicated by white-filled arrows adjacent to both the intact junction (+) and dislodged anular-endplate fragment (*). Before rupture, the separated regions marked by arrows 1 and 2 would have been connected. IV, indicates inferior vertebra; PL, posterior longitudinal ligament. Segment 7–4-L56 is shown.

Figure 8. Circumferentially, the endplate portion of the radial anular-endplate ruptures generally extended farther than the anular portion. In this posterior cryosection of segment 7–1-L56, the endplate rupture, outlined in residual gel (+) and containing nuclear material (*), is sill prominent, whereas the anulus is largely intact. SV indicates superior vertebra; IV, inferior vertebra; DP, disc periphery; N, nucleus.

In order to induce herniation, various methods of flexion have been used. Flexing specimens in an oblique sagittal plane, thus loading one posterolateral aspect of the disc more than the other, has been a popular choice.[3,8,9,11]

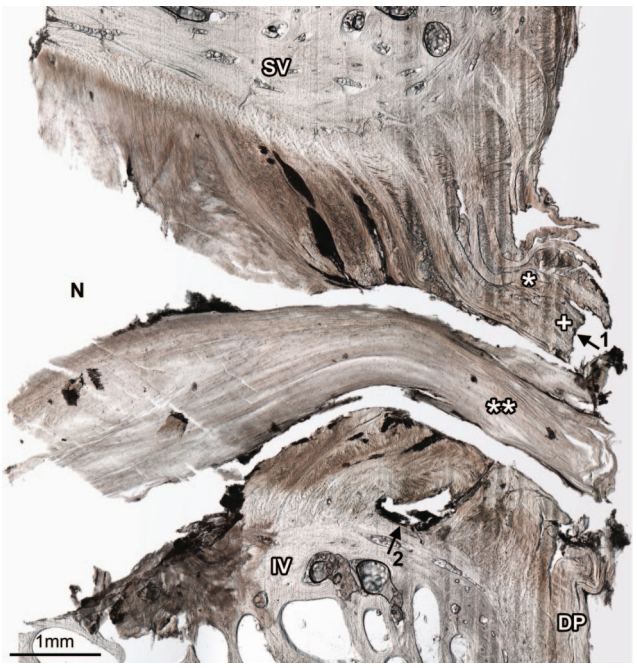

Figure 9. In segment 10–14-L56 a large volume of nuclear material (**) has swept the unanchored portion of anulus (*), along with its attached endplate (+), out beyond the disc periphery (DP). Before rupture, the separated regions marked by arrows 1 and 2 would have been connected. SV indicates superior vertebra; IV, inferior vertebra; N, nucleus.

Because the direction of nuclear tracking and axis of bending may have an approximately orthogonal relationship,[11] and roughly half of the radial tears associated with symptomatic herniations traverse the central posterior anulus,[20,21] flexion was conducted about an axis parallel to the transverse plane in this study. Our findings support those of Aultman *et al*[11]; radial ruptures always occurred in the central posterior anulus, perpendicular to the axis of bending.

In order to halt nuclear pressurization immediately if a focal change to the disc's periphery occurred, the posterior elements of each spine were removed allowing the posterior anulus to be observed. The zygapophysial (facet) joints of lumbar motion segments have been shown to play a significant role in resisting flexion.[32] In order to strain the fibers of the anulus in a reasonably physiologic manner during flexion, a fixed axis of rotation was imposed on segments, approximating the instantaneous axes calculated for upright-standing to full-flexion movements *in vivo*.[33,34]

Previous *in vitro* herniation studies have typically used flexion angles in excess of those that normally occur in the human lumbar spine.[3,8,9,14,15] During the transition from erect standing to a toe-touching posture, an average healthy person will experience between 8° and 14° of flexion at each lumbar level.[3,35] Like Gordon *et al*,[10] we too wanted to use levels of flexion that the lumbar spine would be subjected to on a regular basis, and thus chose to test segments at angles of 7° and 10°.

Nuclear inflation has been used previously to modulate intradiscal pressure in lieu of direct compression.[26,27,36,37] Using this technique, Veres *et al* explored how neutrally positioned ovine lumbar discs fail under hydrostatic pressure.[26] In the current study, we have employed the same inflationary techniques used by Veres *et al*, thus allowing a direct comparison of discs pressurized in the neutral and flexed positions, and subsequent assessment of how flexion affects the disc's ability to resist rupture.

Flexion reduces the disc's ability to withstand high nuclear pressure. Disc failure in the 10° flexion group occurred at a mean pressure of 9.8 MPa, significantly lower than the mean anular failure pressure of 13.2 MPa for discs previously inflated while in the neutral position ($P = 0.02$).[26] This same statistic was not significant for the 7° disc failure group, however, remained significant if the 7° and 10° groups were paired ($P = 0.03$).

In vivo intradiscal pressures range from 0.10 MPa while lying supine, to 2.30 MPa while lifting 20 kg in torso-flexion.[38] While a failure pressure of 10 MPa may seem unphysiologically high, during a fall or jolt involving large magnitudes of deceleration, intradiscal pressures could conceivably reach this level. For example, given that an intradiscal pressure of 2 MPa is generated when a compression load of 2 kN is applied to an average nondegenerate L4–L5 motion segment,[39] the 8.7 kN compressive force routinely experienced by the L4–L5 segment of players during an American football "blocking" maneuver would result in an intradiscal pressure of 10.9 MPa.[40]

Being positioned in flexion has a drastic effect on how a disc ruptures when hydrostatically overloaded. Compared to those discs previously inflated while in the neutral position,[26] the results of this study show that flexion facilitates the flow of nuclear material, and limits circumferential disruption while promoting radial rupture. These observations can be explained as follows. In flexion, the nucleus is pushed posteriorly,[41–43] thereby decreasing the chance of an inner anterior anular rupture when the nucleus becomes hydrostatically pressurized. Conversely, the inner posterior anulus, which when unflexed is known to be the most vulnerable region of the inner anulus,[26] is placed at greater risk of rupture. When the inner posterior anulus ruptures, the posterior force acting on the nucleus facilitates nuclear flow.

In a neutrally position disc, viscous gel flow through the inner and mid-anulus occurs preferentially within adjacent anular fiber bundles, forming circumferential disruptions within lamellae.[26,36] In flexed discs, the fiber bundles making up the posterior anulus would be elongated, and therefore of a reduced diameter, which would increase the flow resistance along their length. As hydrostatic stress in a flexed disc is less readily distributed circumferentially, once the inner posterior anulus has been penetrated intradiscal pressure is relieved more frequently by a radial rupture than diffuse anular failure (Table 2).

We have used the word "acute" in the title of this article to describe our herniations because they have been produced using a single load application rather than cyclic loading. Adams and Hutton[9] noted that herniations produced using flexion and a single application of compressive load differed from those produced using flexion combined with cyclic compression. Those produced cyclically tended to extrude small amounts of nuclear material that had traversed the anular wall in a meandering fashion. Tampier *et al*[14] found that discs which were lightly compressed and cyclically flexed underwent a similar mode of disc herniation. Interestingly, this group noted that nuclear material had wound its way through the anular wall by flowing within anular fiber bundles. In the current study, a straight-line radial rupture was the most common cause of disc failure. We agree with Adams and Hutton[9] that progressive and acute herniations are likely distinct in their morphologies.

Unlike our previously inflated neutral discs,[26] endplate disruption occurred frequently among both flexion groups. Endplate disruption occurred in two forms: rim fractures and radial anular-endplate ruptures. Rim fractures were generally centered on, and symmetric about, the sagittal plane, and had propagated radially at the cortical/cancellous junction (Figure 1). These features are similar to those of a Type II avulsion or limbus fracture described by Takata *et al*[44] and Epstein.[45] Given that patients presenting with rim fractures clinically of-

ten have a history of trauma,[45] it is possible that flexion plays a role in the development of these lesions.

Radial anular-endplate rupture was the most common mode of disc failure to occur. These ruptures displayed a consistent subset of the morphologic characteristics that symptomatic herniations frequently exhibit,[19–21] and therefore may be morphologic signatures of an acute flexion-related injury. These ruptures always occurred in the central posterior anulus and, after starting in the mid-axial plane, tracked towards one endplate, most often the inferior, as they moved radially outwards (Table 1). Endplate rupture, which was located adjacent to the narrowest portion of the anulus, always occurred at the cartilaginous/vertebral endplate junction (Figure 7), allowing the possibility of endplate and/or anulus to be extruded in addition to nuclear material (Figure 9).

The anulus-endplate-anulus failure pattern that most radial ruptures displayed shows how the relative strength of a healthy disc's posterior components vary with radial location (Figures 6 and 9). This same failure pattern has also been observed by Green *et al*,[46] who performed ultimate tensile strength tests on vertebra-disc-vertebra blocks. Green *et al* found that inner anular blocks failed in the mid-axial plane, while blocks from the outer anulus underwent a primary and then secondary failure. Failure first occurred along the inner half of blocks at the endplate/vertebra junction, approximately adjacent to the mid-anulus. The outer 1 to 2 mm of the disc continued to bear load after this initial failure, and eventually the anulus failed in the mid-axial plane.

Both Inoue and Hashizume have documented that fibers from the outer two-thirds of the anulus anchor into the vertebral bodies.[47,48] On the other hand, Francois has advocated that anular fibers are secured to the vertebral rim indirectly *via* calcified cartilage, and do not penetrate the vertebral bodies.[49–51] Our micrographs are not of sufficient detail to confirm the presence of anular fibers penetrating the vertebral bodies. Regardless of how the outer two-thirds of posterior anulus' lamellae are anchored, our results and those of Green *et al*[46] indicate that the outer one-third of the anular/vertebral junction is most robust—more so than the lamellae it secures.

The vertebrae of humans and sheep develop in different ways. While vertebral growth occurs between the cartilaginous endplates and vertebrae in humans, it does not in sheep.[52] It is not unreasonable to suspect that relative to the adjacent anulus, differences in the strength of the endplate junctions may therefore exist between species. The most interesting and reassuring point given the similarity in failure mode transition with radial location observed by ourselves and Green *et al*,[46] is that their study was conducted on human discs. Therefore, despite the differences in vertebral development between these two species, the relative strength between anular and endplate components varies systematically in a similar manner.

The use of nuclear pressurization to modulate intradiscal pressure has proved to be extremely sensitive in allowing us to determine the effects that different postures have on the intervertebral disc's response to hydrostatically imposed stress. Using an ovine lumbar model has provided a consistent reliable supply of healthy tissue—essential to the success of the study. Despite the fact that this study has not been carried out using human tissue, we believe that these are the first clinically relevant *in vitro* herniations to be fully documented.

■ Key Points

- Flexion limits circumferential disruption while promoting radial rupture of the central posterior anulus by pressurized nuclear material.
- The mid-anulus is stronger than its adjacent endplate/vertebrae connections, which are at increased risk of failure when a disc is flexed.
- The outer anulus is weaker than its adjacent endplate/vertebrae connections.
- Flexion may play a developmental role in those herniations possessing a central posterior radial rupture that incorporates a short span of endplate disruption along the apex of the vertebral rim.
- The relative strength between anular and endplate components varies systematically with radial location in a similar manner within the posterior disc wall of both sheep and humans.

Acknowledgment

For the award of grants in support of this research, the authors thank Medtronic Australasia, the New Zealand Orthopedic Association Wishbone Trust, and Education New Zealand.

References

1. Barr JS. "Sciatica" caused by intervertebral-disc lesions. *J Bone Joint Surg Am* 1937;19:323–42.
2. Love JG, Camp JD. Root pain resulting from intraspinal protrusion of intervertebral discs. *J Bone Joint Surg Am* 1937;19:776–804.
3. Adams MA, Hutton WC. Prolapsed intervertebral disc: a hyperflexion injury 1981 Volvo Award in Basic Science. *Spine* 1982;7:184–91.
4. Lin HS, Liu YK, Adams KH. Mechanical response of the lumbar intervertebral joint under physiological (complex) loading. *J Bone Joint Surg Am* 1978;60:41–55.
5. Roaf R. A study of the mechanics of spinal injuries. *J Bone Joint Surg* 1960; 42-B:810–23.
6. Brown T, Hansen RJ, Yorra AJ. Some mechanical tests on the lumbosacral spine with particular reference to the intervertebral discs; a preliminary report. *J Bone Joint Surg Am* 1957;39-A:1135–64.
7. Rolander SD, Blair WE. Deformation and fracture of the lumbar vertebral end plate. *Orthop Clin North Am* 1975;6:75–81.
8. McNally DS, Adams MA, Goodship AE. Can intervertebral disc prolapse be predicted by disc mechanics? *Spine* 1993;18:1525–30.
9. Adams MA, Hutton WC. Gradual disc prolapse. *Spine* 1985;10:524–31.
10. Gordon SJ, Yang KH, Mayer PJ, et al. Mechanism of disc rupture: a preliminary report. *Spine* 1991;16:450–6.
11. Aultman CD, Scannell J, McGill SM. The direction of progressive herniation in porcine spine motion segments is influenced by the orientation of the bending axis. *Clin Biomech (Bristol, Avon)* 2005;20:126–9.
12. Callaghan JP, McGill SM. Intervertebral disc herniation: studies on a porcine

model exposed to highly repetitive flexion/extension motion with compressive force. *Clin Biomech (Bristol, Avon)* 2001;16:28–37.
13. Drake JD, Aultman CD, McGill SM, et al. The influence of static axial torque in combined loading on intervertebral joint failure mechanics using a porcine model. *Clin Biomech (Bristol, Avon)* 2005;20:1038–45.
14. Tampier C, Drake JD, Callaghan JP, et al. Progressive disc herniation: an investigation of the mechanism using radiologic, histochemical, and microscopic dissection techniques on a porcine model. *Spine* 2007;32:2869–74.
15. Kuga N, Kawabuchi M. Histology of intervertebral disc protrusion: an experimental study using an aged rat model. *Spine* 2001;26:E379–84.
16. Fardon DF, Milette PC. Nomenclature and classification of lumbar disc pathology. Recommendations of the Combined task Forces of the North American Spine Society, American Society of Spine Radiology, and American Society of Neuroradiology. *Spine* 2001;26:E93–113.
17. Ohshima H, Hirano N, Osada R, et al.. Morphologic variation of lumbar posterior longitudinal ligament and the modality of disc herniation. *Spine* 1993;18:2408–11.
18. Yasuma T, Makino E, Saito S, et al. Histological development of intervertebral disc herniation. *J Bone Joint Surg Am* 1986;68:1066–72.
19. Moore RJ, Vernon-Roberts B, Fraser RD, et al. The origin and fate of herniated lumbar intervertebral disc tissue. *Spine* 1996;21:2149–55.
20. Maezawa S, Muro T. Pain provocation at lumbar discography as analyzed by computed tomography/discography. *Spine* 1992;17:1309–15.
21. Ninomiya M, Muro T. Pathoanatomy of lumbar disc herniation as demonstrated by computed tomography/discography. *Spine* 1992;17:1316–22.
22. Harada Y, Nakahara S. A pathologic study of lumbar disc herniation in the elderly. *Spine* 1989;14:1020–4.
23. Willburger RE, Ehiosun UK, Kuhnen C, et al. Clinical symptoms in lumbar disc herniations and their correlation to the histological composition of the extruded disc material. *Spine* 2004;29:1655–61.
24. Mundt DJ, Kelsey JL, Golden AL, et al; The Northeast Collaborative Group on Low Back Pain. An epidemiologic study of non-occupational lifting as a risk factor for herniated lumbar intervertebral disc. *Spine* 1993;18:595–602.
25. Seidler A, Bolm-Audorff U, Siol T, et al. Occupational risk factors for symptomatic lumbar disc herniation: a case-control study. *Occup Environ Med* 2003;60:821–30.
26. Veres SP, Robertson PA, Broom ND. Microstructure and mechanical disruption of the lumbar disc annulus. Part II: how the annulus fails under hydrostatic pressure. *Spine* 2008;33:2711–20.
27. Schechtman H, Robertson PA, Broom ND. Failure strength of the bovine caudal disc under internal hydrostatic pressure. *J Biomech* 2006;39:1401–9.
28. Wilke HJ, Kettler A, Wenger KH, et al. Anatomy of the sheep spine and its comparison to the human spine. *Anat Rec* 1997;247:542–55.
29. Smit TH. The use of a quadruped as an in vivo model for the study of the spine–biomechanical considerations. *Eur Spine J* 2002;11:137–44.
30. Wilke HJ, Kettler A, Claes LE. Are sheep spines a valid biomechanical model for human spines? *Spine* 1997;22:2365–74.
31. Reid JE, Meakin JR, Robins SP, et al. Sheep lumbar intervertebral discs as models for human discs. *Clin Biomech (Bristol, Avon)* 2002;17:312–4.
32. Adams MA, Hutton WC, Stott JR. The resistance to flexion of the lumbar intervertebral joint. *Spine* 1980;5:245–53.
33. Yoshioka T, Tsuji H, Hirano N, et al. Motion characteristic of the normal lumbar spine in young adults: instantaneous axis of rotation and vertebral center motion analyses. *J Spinal Disord* 1990;3:103–13.
34. Pearcy MJ, Bogduk N. Instantaneous axes of rotation of the lumbar intervertebral joints. *Spine* 1988;13:1033–41.
35. Pearcy M, Portek I, Shepherd J. Three-dimensional x-ray analysis of normal movement in the lumbar spine. *Spine* 1984;9:294–7.
36. Pezowicz CA, Schechtman H, Robertson PA, et al. Mechanisms of annular failure resulting from excessive intradiscal pressure: a microstructural-micromechanical investigation. *Spine* 2006;31:2891–903.
37. Jayson MI, Herbert CM, Barks JS. Intervertebral discs: nuclear morphology and bursting pressures. *Ann Rheum Dis* 1973;32:308–15.
38. Wilke HJ, Neef P, Caimi M, et al. New in vivo measurements of pressures in the intervertebral disc in daily life. *Spine* 1999;24:755–62.
39. Adams MA, McNally DS, Dolan P. "Stress" distributions inside intervertebral discs: the effects of age and degeneration. *J Bone Joint Surg Br* 1996;78:965–72.
40. Gatt CJ Jr, Hosea TM, Palumbo RC, et al. Impact loading of the lumbar spine during football blocking. *Am J Sports Med* 1997;25:317–21.
41. Fennell AJ, Jones AP, Hukins DW. Migration of the nucleus pulposus within the intervertebral disc during flexion and extension of the spine. *Spine* 1996;21:2753–7.
42. Alexander LA, Hancock E, Agouris I, et al. The response of the nucleus pulposus of the lumbar intervertebral discs to functionally loaded positions. *Spine* 2007;32:1508–12.
43. Seroussi RE, Krag MH, Muller DL, et al. Internal deformations of intact and denucleated human lumbar discs subjected to compression, flexion, and extension loads. *J Orthop Res* 1989;7:122–31.
44. Takata K, Inoue S, Takahashi K, et al. Fracture of the posterior margin of a lumbar vertebral body. *J Bone Joint Surg Am* 1988;70:589–94.
45. Epstein NE. Lumbar surgery for 56 limbus fractures emphasizing noncalcified type III lesions. *Spine* 1992;17:1489–96.
46. Green TP, Adams MA, Dolan P. Tensile properties of the annulus fibrosus. Part II: ultimate tensile strength and fatigue life. *Eur Spine J* 1993;2:209–14.
47. Hashizume H. Three-dimensional architecture and development of lumber intervertebral discs. *Acta Med Okayama* 1980;34:301–14.
48. Inoue H. Three-dimensional architecture of lumbar intervertebral discs. *Spine* 1981;6:139–46.
49. Francois RJ. Ligament insertions into the human lumbar vertebral body. *Acta Anat (Basel)* 1975;91:467–80.
50. Francois RJ. Three-dimensional architecture of lumbar intervertebral discs. *Spine* 1982;7:522–3.
51. Francois RJ, Bywaters EG, Aufdermaur M. Illustrated glossary for spinal anatomy: with explanations and a French and German translation. *Rheumatol Int* 1985;5:241–5.
52. Alini M, Eisenstein SM, Ito K, et al. Are animal models useful for studying human disc disorders/degeneration? *Eur Spine J* 2008;17:2–19.